published in Environmental Chemistry 12 (2015) 112–122

Interpretation of DGT measurements. Review of a systematic approach.

Josep Galceran* and Jaume Puy

Departament de Química, Universitat de Lleida and AGROTECNIO. Rovira Roure 191, 25198 Lleida, Spain

* corresponding author, galceran@quimica.udl.cat

Environmental Context

Dynamic speciation of a given element in a natural medium is key for understanding its availability. DGT has become a widely used tool for in-situ environmental studies, being applied to determine fluxes of metal cations (Zn, K, Fe..), anions (such as phosphate), organics, antibiotics, nanoparticles, etc.. The interpretation of the measurements with suitable physicochemical models gives valuable insights on the behavior of the system.

Abstract

Gaining insight into the physicochemical processes integrated in a DGT (Diffusion Gradients in Thin Films) measurement and combining them in a model can assist in retrieving fundamental information, both qualitative and quantitative, on the probed system. New experiments (such as varying the thicknesses of the gel and/or the resin layer) and their mathematical treatment to extract meaningful parameters have been suggested from theoretical considerations. The concept of lability degree is useful in describing an interpretation of the DGT-concentration as the summation of the free metal concentration plus the labile fraction of all complexes multiplied by a ratio of diffusion coefficients. In some cases, the lability degree can be directly estimated with specific measurements and a very simple expression. We review the current status of these interpretations, including numerical simulations, with special focus on analytical expressions, because they can be more accessible to the standard DGT practitioner. Present limitations and challenges for future work in DGT interpretation are also discussed.

1. Introduction

Since its presentation in 1994,[1] DGT (Diffusive Gradients in Thin Films) has reached an extraordinary success in the scientific community working in environmental speciation and availability. There are many reasons for this success, from its simple conceptual design to the practical availability of accurately manufactured devices. The amplitude of applications[2] arises not only from the variety of media (waters,[3] sediments,[4,5] soils,[6] etc.), but also from the variety of analytes (heavy metals,[7,8] lanthanides,[9,10] K,[11] phosphate,[12,13] As, V, Sb, Mo, W,[14] Fe,[15] nanoparticles,[16,17] antibiotics,[18]..) and also from its designed *in situ* measurement capacity.[19]

Theoretical contributions have also been developed[20-25] to interpret the measurements and even have been able to suggest new experiments to gain more information about the probed system. Numerical models, analytical expressions and experimental approaches complement and reinforce each other helping in unraveling the system characteristics. However, any model is a simplification of the reality. So it is essential to judiciously choose the most relevant phenomena and neglect the rest, keeping a balance between simplicity (few selected phenomena, simpler geometries, limiting regimes, etc.) and sufficient accuracy in the predicted response. For instance, the resin layer is in reality a 3D entity with resin beads tending to be denser close to the resin/gel interface (due to the settling preparation of the resin layer), but analytical expressions could not be derived for such a 3D model.

Here, we review a DGT interpretation which essentially relies on physicochemical modeling of diffusion and complex dissociation. The primary environmental context in mind corresponds to heavy metals in aqueous media, but other media (such as soil or sediments) or other analytes could also be considered.

The structure of this work is as follows. In section 2, the direct information provided by accumulation and fluxes is linked to the concept of lability degree. This will allow an interpretation of the DGT-concentration in section 3. Section 4 considers the "Penetration Analytical Model", PAM, which is progressively extended to include mixtures (section 5), the diffusive boundary layer (section 6) or electrostatic effects (section 7). Limitations and prospects are briefly suggested in section 8.

2. Key concepts: accumulation, fluxes and lability degree

A DGT device consists of a resin layer (with thickness r), covered with a diffusive gel layer (of thickness g) and a filter in contact with the probed phase (in principle, aqueous solution in this work) where a diffusive boundary layer, DBL (of thickness δ) can develop. Let n_M be the number of moles of the analyte (M for simplicity) accumulated in the resin at a given time (t). The flux, can be computed as:

$$J(t) = \frac{1}{A}\frac{dn_M}{dt} \quad (1)$$

where A is the effective area of the gel-solution interface. A detailed plot of the accumulated n_M in front of increasing deployment times would reveal 4 regimes: transient (when the flux is growing), (quasi) steady-state regime (practically constant flux), approach to equilibrium (decreasing flux) and equilibrium (null flux)[26,27]. The practical use of DGT has consisted in focusing in the steady-state regime (while neglecting the very small effects of the short transient regime), so that, the time integral of the flux becomes just

$$n_M = JAt \quad (2)$$

Thus, from the processing of the accumulations, DGT is also providing a quantification of the flux.

This steady-state flux will result from the contributions by the arrival of free M and other M-containing species to the sensor. For simplicity, let us start assuming that just one complex ML is formed with a ligand L:

$$\mathrm{M} + \mathrm{L} \underset{k_d}{\overset{k_a}{\rightleftharpoons}} \mathrm{ML} \tag{3}$$

The stability constant K (ratio of the association and dissociation kinetic constants, k_a and k_d) rules the concentration in the bulk (denoted with superscript *) of the sampled solution:

$$K = \frac{k_a}{k_d} = \frac{c^*_{ML}}{c^*_M c^*_L} \tag{4}$$

For vanishing values of the rate constants, the inert complex does not dissociate and the free metal J_{free} would be the only contribution to the total flux. For extremely high values of the rate constants, metal and complex are in equilibrium at all points and the resulting flux (J_{lab}) is termed fully labile. The extent of the participation of the complex to the total flux can be quantified by the lability degree ξ[28] of the complex:

$$\xi \equiv \frac{J - J_{free}}{J_{labile} - J_{free}} \tag{5}$$

With this definition, ξ=0 for an inert complex and ξ=1 for a fully labile one.

It can be shown[28,29], that, for systems with only one ligand and vanishing concentration of M at the resin-gel interface (x=r), the lability degree is directly connected to the normalized concentration of ML at that point:

$$\xi = 1 - \frac{c^r_{ML}}{c^*_{ML}} \tag{6}$$

where the superscript r indicates the concentration of ML at x=r.

From the definition of ξ (5),

$$J = J_{\text{free}} + \xi\left(J_{\text{labile}} - J_{\text{free}}\right) \tag{7}$$

For trace speciation measurements, usually J_{free} is negligible as the amount of free metal is very low (one could label this as "overwhelming complex" conditions). Under these conditions, and if the diffusion coefficient of the complex is known or can be estimated, one can compute the lability degree as:

$$\xi \approx \frac{J}{J_{\text{labile}}} \approx \frac{n_{\text{M}} / (At)}{\left(\frac{D_{\text{ML}}}{D_{\text{M}}}\right) n_{\text{M}}^{no-ligand} / (At)} = \frac{D_{\text{M}}\, n_{\text{M}}}{D_{\text{ML}}\, n_{\text{M}}^{no-ligand}} \tag{8}$$

where the labile flux has been estimated from the accumulation of M in the same system, but without ligand (i.e. just the metal) and a re-scaling by a factor to take into account the different diffusion coefficients of the complex (D_{ML}) and of the metal (D_{M}). In this sense, the lability degree can be interpreted as a normalised flux (where diffusion coefficients and not only accumulated amounts are involved).

The definition of a global lability degree (5) can be extended to a system with any number of ligands, and can be approximated with eqn. (8) if all complexes have a similar diffusion coefficient D_{ML}.

3. What is DGT-concentration?

From the steady-state solution of Fick's second law for just one species in planar geometry, and assuming that the concentration of this species M vanishes at the resin-gel interface, the simple expression[1] follows

$$n_{\text{M}} = A\left(\frac{D_{\text{M}}\, c_{\text{DGT}}}{g}\right) t \tag{9}$$

(where the thickness of the gel g could include the filter and DBL thickness in some cases[2]). Provided that the diffusion coefficient of free metal is used for D_M in eqn. (9), this can be taken as an operational definition of the DGT-concentration, c_{DGT}. Its physical meaning is quite simple: c_{DGT} is the metal concentration needed in an only-M system to obtain the same flux as in the system under study (where usually there are complexes which also contribute to the flux by dissociation).

Let us now consider a system with h ligands (denoted from ^1L to ^hL) that can form h complexes. It can be shown -see eqn. (SI-21) in the Supporting Information of [30]- that, when M vanishes at $x=r$, the total flux can be formally written as

$$J = \frac{D_M c_M^*}{g} + \sum_{j=1}^{h}\left[\frac{D_{M^jL} c_{M^jL}^*}{g}\left(1 - \frac{c_{M^jL}^r}{c_{M^jL}^*}\right)\right] = \frac{D_M c_M^* + \sum_j \xi_j D_{M^jL} c_{M^jL}^*}{g} \quad (10)$$

where

$$\xi_j \equiv 1 - \frac{c_{M^jL}^r}{c_{M^jL}^*} \quad (11)$$

is labeled as the lability degree of the complex M^jL.[31]

Comparison of eqn. (9) and (10) allows to solve for c_{DGT} :

$$c_{DGT} = c_M^* + \sum_j \xi_j \frac{D_{M^jL}}{D_M} c_{M^jL}^* \quad (12)$$

which provides an interpretation of c_{DGT} in terms of the species present in the system: each species contributes to c_{DGT} with the equivalent free metal that gives the same contribution to the metal flux.

Notice that previous expressions hold even in the absence of ligand excess ($c^*_{\mathrm{M}^j\mathrm{L}} >> c^*_{\mathrm{M}}$)[29].

Now, if we assume that all diffusion coefficients are similar and that complexes can be just classified as either totally inert (ξ=0) or fully labile (ξ=1), one finds

$$c_{\mathrm{DGT}} \approx c^*_{\mathrm{M}} + \sum_{k}^{\textit{fully labile}} c^*_{\mathrm{M}^k\mathrm{L}} \qquad (13)$$

which supports the basic notion that DGT is essentially measuring the labile fraction of the complexes[2,32-34].

However, more rigorously, eqn. (12) indicates that c_{DGT} is the sum of labile concentrations *weighted* by the ratios of each complex diffusion coefficient with respect to D_{M} [22,33,35]. So one must resist the temptation of attributing all variations in c_{DGT} just to lability, while disregarding changes in mobility. As an example, consider a system with just one fully labile complex (ξ=1) with low mobility (D_{ML}=0.01 D_{M}) at a bulk concentration overwhelming with respect to the free concentration $\left(\frac{D_{\mathrm{ML}}}{D_{\mathrm{M}}} c^*_{\mathrm{ML}} >> c^*_{\mathrm{M}} \right)$.

According to eqn. (12), an experiment could yield $c_{\mathrm{DGT}} = 0.01\, c^*_{\mathrm{ML}}$ even though the complex is labile. So, the retrieved c_{DGT} is not just the true labile concentration (which we know it is c^*_{ML}), but the labile concentration times the ratio of the complex over metal diffusion coefficient. One could even find cases where the diffusion coefficient of the formed complex is higher than the one of just metal (i.e. such as iodide with cadmium [36]) and obtain a DGT-concentration higher than the total one (i.e. $c_{\mathrm{DGT}} > c^*_{\mathrm{ML}} \approx c^*_{\mathrm{T,M}}$). Table 1 considers 4 cases with the same total metal, free metal and DGT concentrations for a mixture of two complexes. In the first 3 combinations, the concentration of both complexes is the same. In the first case, the contribution of both complexes to c_{DGT} is the

same, although complex 1 is only half-labile and mobile, while complex 2 is fully labile but just half-mobile. In the second case, only complex 1 contributes, because M^2L is immobile. In the third case, only complex 2 contributes, because M^1L is totally inert. In case 4, we have $c^*_{M^2L} > c^*_{M^1L}$, but the contribution of the "super-mobile" complex 1 is higher than the one of the quite immobile complex 2, whose labile fraction (5.74 nM) is also higher than c_{DGT} (5.02 nM).

The use of c_{DGT} as the output of the DGT experiment has simplified the practical manipulation of the result, while the high correlation between this measurement and toxicity or availability experiments[37] has boosted the popularity of DGT. This correlation also indicates that fluxes play a key role in uptake or toxicity phenomena.[38]

4. Penetration of the complex into the resin layer

The prediction of the flux in a system with just one complex taking into account the kinetics of association/dissociation was initially based on assuming that the resin acted as a "perfect sink" for the metal (i.e. c_M=0 for x<=r) and "perfect wall" for the complex (i.e. null flux of ML at x=r). The so-called "voltammetric expressions"[39] failed to reproduce the experimental results[40].

More refined numerical models[22,24,41] introduced a new phenomenon: both M and ML can diffuse in the resin layer (still considered ideally as a 1D domain with binding sites evenly distributed). Due to "penetration", the reaction layer, i. e., the layer where there is net dissociation of the complex, extends from the gel domain into the resin domain, this having a high impact on metal accumulation. These numerical models successfully fitted the experimental results. They also led to the derivation of a simplified analytical model[41] with the help of additional hypotheses such as: i) perfect sink for M throughout

194 the resin layer (backed with experimental observations in [42,43]), and ii) excess of ligand
195 L (i.e. the bulk concentration of M is much less than that of ML). The expressions of the
196 analytical model reproduced the experimental results as the numerical simulations
197 whenever the additional hypotheses held. Characteristic indicators of the penetration
198 analytical model (PAM) are the penetration parameter λ_{ML} and the disequilibration layer
199 thickness *m*.

200 $$\lambda_{ML} = \sqrt{\frac{D_{ML}}{k_d}} \quad (14)$$

201 is related to the distance of penetration of ML inside the resin. It can be seen as the
202 intercept of the tangent of c_{ML}-profile at $x=r$ with the abscissae axis (i.e. zero ML
203 concentration) and it is related to the thickness of the reaction layer in the resin domain.

204 $$m = \sqrt{\frac{D_{ML}}{k_d\left(1+\varepsilon K'\right)}} \quad (15)$$

205 is a quantification of the thickness (within the gel phase) where c_M and c_{ML} are not in
206 equilibrium in terms of the effective stability constant (i.e. the reaction layer in the gel
207 domain),

208 $$K' = Kc_L^* \quad (16)$$

209 and the normalized diffusion coefficient

210 $$\varepsilon = \frac{D_{ML}}{D_M} \quad (17)$$

211 The flux can be expressed as

212 $$J = \frac{D_M c_M^*}{g} + \frac{D_{ML} c_{ML}^*}{g}\xi = \frac{D_M c_M^*}{g}\left(1+\varepsilon K'\xi\right) \quad (18)$$

213 with the lability degree being

$$\xi = 1 - \frac{c_{ML}^{r}}{c_{ML}^{*}} = 1 - \frac{\left(1+\varepsilon K^{'}\right)}{\varepsilon K^{'} + \frac{g}{m}\coth\left(\frac{g}{m}\right) + \frac{g}{\lambda_{ML}}\left(1+\varepsilon K^{'}\right)\tanh\left(\frac{r}{\lambda_{ML}}\right)} \quad (19)$$

The availability of analytical expressions within PAM for the flux, the lability degree, the concentrations profiles, etc. allows gaining insights into the impact of the various physicochemical parameters. The plotting of the concentration profiles (such as those seen in Fig 1) allows one to visualize regions where equilibrium is practically fulfilled as the zones where the normalized concentrations collapse. In the shown case of CoNTA, the collapse almost reaches the interface resin/gel, reflecting a quite labile complex as also confirmed by the low value of c_{ML}^{r} (see eqn. (6)).

Previous studies, using PAM, have shown:

i) Neglecting penetration (e.g. using voltammetric expressions[39]), seriously underestimates the lability of the complex [40] or, in other words, the penetration into the resin *labilizes* the complex (i.e. DGT senses a much more labile fraction than voltammetric techniques).

ii) The change in the value *g* (around typical values) has a mild impact on *J* and on ξ ,[41,44]

iii) The influence of the ligand concentration on the lability degree is mild (for ligand excess conditions).[27,30]

iv) The variation of *r* can have a large effect[40,41] and future experimental designs with resins of varying thickness are expected to further exploit this fact.

Experiments with 2 resin layers (also called double binding layers), denoted “back” and “front”, have already been used to probe the complex dissociation rates.[43,45] Information gained from analytical expressions can be helpful not only as experimental guidelines,

but also for the numerical simulations (given the vast number of combination of parameters that might be necessary to explore to reach certain conclusions). For instance, with the PAM, and following a similar procedure to that used in ref. [42] for just metal, one can derive rigorous and approximate expressions for multilayer accumulations as shown next.

The number of moles accumulated in the front resin (extending from $x=r/2$ to $x=r$) can be computed as

$$n_{\mathrm{M}}^{\mathrm{Front}} = tA\int_{r/2}^{r} k_{\mathrm{d}} c_{\mathrm{ML}}(x)\,dx + tAD_{\mathrm{M}} \left.\frac{dc_{\mathrm{M}}}{dx}\right|_{x=r} \tag{20}$$

and the moles in the back resin is

$$n_{\mathrm{M}}^{\mathrm{Back}} = tA\int_{0}^{r/2} k_{\mathrm{d}} c_{\mathrm{ML}}(x)\,dx \tag{21}$$

where the entire flux of free metal arriving to the resin is assigned to the front layer. For the first right hand term of $n_{\mathrm{M}}^{\mathrm{Front}}$ and for $n_{\mathrm{M}}^{\mathrm{Back}}$, integration is very easy because (see SI - 9 in ref. [41])

$$c_{\mathrm{ML}}(x<r) = c_{\mathrm{ML}}^{r}\frac{\cosh\left(\frac{x}{\lambda_{\mathrm{ML}}}\right)}{\cosh\left(\frac{r}{\lambda_{\mathrm{ML}}}\right)} \tag{22}$$

The flux of metal at the interphase (second term in the right hand side of (20)) can be computed combining SI-24 and SI-25 in ref. [41]. Thus, after simple algebra using c_{ML}^{r} given by eqn. SI-27 in ref. [41], only finally reaches

$$\frac{n_{\mathrm{M}}^{\mathrm{Front}}}{n_{\mathrm{M}}^{\mathrm{Back}}} = 2\cosh\left(\frac{r}{2\lambda_{\mathrm{ML}}}\right) - 1 + \left[\frac{\lambda_{\mathrm{ML}}}{m\varepsilon K'}\coth\left(\frac{g}{m}\right) + \frac{1}{\varepsilon K'}\tanh\frac{r}{\lambda_{\mathrm{ML}}}\right]\frac{\cosh\left(\frac{r}{\lambda_{\mathrm{ML}}}\right)}{\sinh\left(\frac{r}{2\lambda_{\mathrm{ML}}}\right)} \tag{23}$$

It can be seen that the term in between the square brackets (corresponding to the contribution of metal dissociation in the gel) is negligible for typical parameter values. So,

$$\frac{n_{\mathrm{M}}^{\mathrm{Front}}}{n_{\mathrm{M}}^{\mathrm{Back}}} = 2\cosh\left(\frac{r}{2\lambda_{\mathrm{ML}}}\right) - 1 \qquad (24)$$

can be seen as a practical accurate simplified expression corresponding to just the dissociation of ML inside each of the two binding resins. Eqn (24) is not a good estimate of eqn. (23) for extremely inert complexes, as in this case the approximation cannot take into account that most of the arriving total metal goes to the front layer (because the dissociation in the resin layer becomes increasingly negligible). The discrepancies for some "pathological" cases can be seen in Fig. 2, where, in order to bound the variations in the range [0..1], the ratio of the front layer over the total amount of moles, $\frac{n_{\mathrm{M}}^{\mathrm{Front}}}{n_{\mathrm{M}}} = \frac{\frac{n_{\mathrm{M}}^{\mathrm{Front}}}{n_{\mathrm{M}}^{\mathrm{Back}}}}{\frac{n_{\mathrm{M}}^{\mathrm{Front}}}{n_{\mathrm{M}}^{\mathrm{Back}}}+1}$ is represented for different λ_{ML} values.

For sufficiently large *r*-values (see cases of Co and Cd in Fig. 3), $\frac{n_{\mathrm{M}}^{\mathrm{Front}}}{n_{\mathrm{M}}}$ tends to one, as λ_{ML} will become much shorter than the thickness of the front resin layer. For intermediate *r*-values, some ML will be able to reach the back resin layer and $\frac{n_{\mathrm{M}}^{\mathrm{Front}}}{n_{\mathrm{M}}}$ can approach 0.5 (especially for very inert complexes). For very small *r*-values, the contribution of ML dissociation in the resin phase will be negligible in front of the dissociation in the gel domain (which is ascribed to bind to the front resin layer). Notice that it is for this small *r*-values that the approximation (24) fails to consider that and it rather tends to $\frac{n_{\mathrm{M}}^{\mathrm{Front}}}{n_{\mathrm{M}}}$ =0.5

For the CdNTA case (orange continuous line), a change in the resin thickness close to the typical value (r=0.4 mm) does not modify the ratio $\frac{n_{\mathrm{M}}^{\mathrm{Front}}}{n_{\mathrm{M}}}$ from a value very close to 1, indicating that almost all metal gets bound at the front resin in agreement to the labile behavior of the CdNTA complex. So, this change cannot be used to find λ_{ML} and the kinetic information on CdNTA. Likewise, for a too inert case, $\frac{n_{\mathrm{M}}^{\mathrm{Front}}}{n_{\mathrm{M}}} \approx 0.5$ and no reliable information other than $\lambda_{\mathrm{ML}} >> r$ can be obtained.

The region of transition from 0.5 to 1 can be quantified via a "characteristic resin thickness" from the ratio attaining the intermediate value 0.75. From $\frac{n_{\mathrm{M}}^{\mathrm{Front}}}{n_{\mathrm{M}}} = 0.75$, using eqn. (24) one finds that this characteristic resin thickness can be around

$$2 \operatorname{arccosh} 2 \lambda_{\mathrm{ML}} \approx 2.63 \lambda_{\mathrm{ML}} \qquad (25)$$

Only the use of double resins whose total thickness is of the order of magnitude of $2 \lambda_{\mathrm{ML}}$ can yield values sufficiently different from 0.5 and 1 as to be used for retrieving kinetic information (taking into account typical experimental errors). In the cases used in Fig3, the λ_{ML} -values are 9.57×10^{-6} m for CdNTA, 2.19×10^{-4}m for CoNTA and 7.14×10^{-2}m for NiNTA. The kinetic parameters of too labile complexes (such as CdNTA) or too inert complexes (such as NiNTA) could not be accurately resolved with ordinary resins (r=4×10^{-4}m).

So, for a given resin thickness, there is a kinetic window of available information for the analysis based on (23) or (24). Conversely, up to certain extent, the thickness of the resin could be tuned[46] to the characteristic resin length of the complex.

Apart from a preliminary exploration [43], the potential practical use of (24) to retrieve the kinetic parameter λ_{ML} has yet to be confirmed with further experiments in systems fulfilling the hypotheses of PAM and overcoming technical difficulties.

5. Mixtures

Environmental samples are practically always a mixture of many components, of both metal ions and ligands, giving rise to a distributed variety of equilibrium constants (hetererogeneity)[44] and diffusion coefficients (polydispersity).

In principle, a *mixture of metal cations* (in combination with a homogeneous ligand) can be dealt with in DGT as if each metal was alone, provided the excess of ligand conditions apply for each one of the elements (i.e. negligible competition effects in the bulk). In this way, the expressions in this work appearing up to here apply to each metal under the corresponding assumptions.

As commented above, expression (10) holds for a *mixture of ligands* that react with a metal in a set of parallel reactions regardless the ligand to metal ratio. The question now is how the mixture impacts on the expression for the particular lability degree of each complex arising in eqn. (10), i.e., can eqn. (19) be used in eqn. (10)?. This question is of high interest, since it would allow studying complex mixtures with information obtained from single ligand systems.

In a mixture of ligands, the diffusion-reaction process of the species related to one ligand, say ^{1}L, is coupled to the diffusion-reaction processes of the species related to all other ligands, because all the reaction systems are coupled through M[31,47,48]. So, a rigorous approach requires numerical simulation. However, under ligand excess conditions with the hypothesis of the resin being a perfect sink for the metal, then c_M becomes zero in the resin phase and the coupling can only affect the gel phase. Within a wide range of

322 explored conditions, digital computations have indicated that the dissociation of
323 complexes mostly occurs in the resin,[30] so that the coupling in the gel domain is very
324 mild. Thus, the rigorous expression (10) for the flux can be approximated, under ligand
325 excess conditions, by replacing each individual lability degree ξ_j in the whole mixture
326 (only accessible via intensive computation) with the lability degree ($\xi_j^{h=1}$) in an equivalent
327 system where there was only the ligand ^{j}L (both ligand and metal at the same total
328 concentrations as the original system).

329 $$J^{h=1} = \frac{D_{\mathrm{M}} c_{\mathrm{M}}^{*} + \sum_{j} \xi_j^{h=1} D_{\mathrm{M}^{j}\mathrm{L}} c_{\mathrm{M}^{j}\mathrm{L}}^{*}}{g} \qquad (26)$$

330 Thus $\xi_j^{h=1}$ can be computed with eqns. such as (19) (if there is no specific DBL to
331 consider) or other more involved equations (if the solution has a very different behavior
332 than the gel phase). This approximation has been shown more accurate than 10% for
333 mixtures with devices having a g thicker than 0.8 mm[30].

334

335 ## 6. Diffusive boundary layer: experiments varying the
336 thickness of the gel layer

337 In fact, since DGT's presentation,[1,32] it was recognized that convective movements in
338 the solution would extend the diffusion domain with a "diffusive boundary layer", DBL.
339 Rigorously speaking, one should take into account the velocity profiles (for the various
340 hydrodynamic regimes which might vary for different zones of solution in the proximity
341 of the filter and for different experiments) and solve the pertaining continuity equation
342 taking into account the flow term (see eqns. (21)-(34) in [49] and refs. [50,51]). Up to now,
343 all treatments of DBL with DGT rely on Nernst diffusion layer concept: they assume that
344 the real system is equivalent (regarding the final flux) to a virtual one where there is full
345 stirring for $x>r+g+\delta$ (i.e. bulk conditions) and quiescent conditions in between $x=r+g$ and

346 $x=r+g+\delta$. This assumption might be especially critical because the "equivalence" for just
347 M can be very different to the required equivalence for another system having also a given
348 M^1L or a third system with a mixture of complexes (e.g. this equivalence might be
349 dependent on the diffusion coefficients of the species presents in the mixture).[49] Future
350 work to establish the impact of the Nernst diffusion layer approximation is timely.
351 All equations presented up to here remain valid in the case of any existing DBL provided
352 that: i) Nernst diffusion layer concept is acceptable, ii) the diffusion coefficients of all
353 species are acceptably similar in the gel and in the solution and iii) there are no Donnan
354 partitioning effects between gel and solution (see section 7); in this case one should use
355 an effective g resulting from the aggregated thicknesses of the gel, filter and DBL
356 thicknesses.
357 Experiments with varying gel thickness have been performed to estimate the physical
358 length of the DBL[32,52,53]. Several works[12,25,50,51,54,55] tackled the determination of δ
359 when $D_M \neq D_M^w$ and/or $D_{ML} \neq D_{ML}^w$ (superscript "w" indicates that the diffusion
360 coefficient correspond to the solution -water phase; no superscript is used here for
361 parameters in the diffusive gel although in the SI of ref [25] the superscript "gel" was used).
362 Imposing continuity of the fluxes and concentrations at the boundary gel-solution, and
363 assuming equilibrium between M and ML in the solution, one arrives (see SI of [25]) to:

364 $$J = \frac{c_M^*}{\frac{\delta}{D_M^w\left(1+\varepsilon^w K^{'}\right)} + \frac{g + g_{kin}^p}{D_M\left(1+\varepsilon\ K^{'}\right)}} \qquad (27)$$

365 where

366 $$g_{kin}^p \equiv \frac{\varepsilon K^{'} m \tanh\frac{g}{m}}{1+\varepsilon K^{'} m\left(\tanh\frac{g}{m}\right)\left(\frac{1}{\varepsilon K^{'}}+1\right)\frac{1}{\lambda_{ML}}\tanh\frac{r}{\lambda_{ML}}} \qquad (28)$$

can be seen as the equivalent extra length that would be necessary to add to the gel layer thickness to account for the decrease of accumulated metal due to the kinetic limitations.[25]

Fig 4 shows that, for the chosen typical parameters, the impact of varying δ on the flux is rather mild, in agreement with experimental reports[51]. As expected, the flux decreases when δ increases or the diffusion coefficients inside the gel decrease.

As seen in Fig 5, lability increases when the DBL thickness increases or the diffusion coefficient D_{ML} decreases in the gel: in both cases there is more "time" along which the complex can dissociate.

The representation of the inverse of the accumulated mass [25,32,33] in front of varying g can be used to experimentally estimate the thickness of the DBL and, more importantly, to find the dissociation rate constant in systems where the bold assumption of just one ligand is acceptable. In the case of penetrating complex, previous eqns. (27) and (28) (see also SI of [25]) can be recast as:

$$\frac{1}{n_M} = \left[\frac{\delta}{D_M^w \left(1+\varepsilon^w K'\right) c_M^* A t} + \frac{g_{kin}^p}{D_M \left(1+\varepsilon\ K'\right) c_M^* A t} \right] + \frac{g}{D_M \left(1+\varepsilon\ K'\right) c_M^* A t} \qquad (29)$$

Strictly speaking, g_{kin}^p is also dependent on g, as eqn. (28) indicates. In cases where this dependence was suspected to be strong, one could fit as free parameters δ, c_M^* and g_{kin}^p in eqn. (29) with at least 3 experimental points of accumulation (i.e. at least 3 pairs (n_M, g)). Then, as g_{kin}^p can be written in terms of k_d (by using eqn. (14) and (15) to replace λ_{ML} and m), the value of k_d can be found.

However, for typical parameters, the dependence of g_{kin}^p on g is mild, whenever $g>2\ m$, because the term $\tanh(g/m)$ tends to 1. For instance, for a rather inert complex such as NiNTA at a total concentration such as K'=60600, k_d=7.710^{-6} s^{-1} (Eigen mechanism),

D_M=7.07×10^{-10} and D_{ML}=0.7×D_M, we compute m=3.8×10^{-5} m which is much less than the usual g. (Notice however, that this m would be larger than the 0.01 mm extra-thin gel layer used in recent developments[46] and whose rigorous treatment would require a modified version of the PAM because there is no equilibrium throughout the DBL, see assumption above equation (27)).

So, in systems with one homogeneous ligand and no further complications, one would expect the representation of $1/n_M$ to be linear with g, as prescribed by eqn. (29) with constant g^p_{kin}. The ratio of the intercept over the slope (obtained in the linear regression) is:

$$\frac{i}{s} = \frac{D_M\left(1+\varepsilon\ K'\right)}{D_M^w\left(1+\varepsilon^w K'\right)}\delta + g^p_{kin} \qquad (30)$$

which allows to find k_d from g^p_{kin} using eqn. (14) and (15) as described above. The representation of the so-called Apparent Diffusive Boundary Layers (i.e. $ADBL = \frac{D_M^w}{D_M}\frac{i}{s}$) for several metals is designated as "kinetic signature" of the mixture .[33]

Fig 6 shows the good linearity that could be obtained in a case of Cd with NTA and Co with NTA. The parallelism between the practically straight lines is due to the similarity of the diffusion coefficients and the K'-values. The linear regression of 3 points (at single, double and triple the standard value of g) of the Co series yielded a ratio i/s= 3.06×10^{-4} m which, applying eqn. (30), yielded g^p_{kin} =2.26×10^{-4} m in full agreement with the directly computed value of g^p_{kin}.

Notice that, in the particular case where the diffusion coefficients in the gel and in the solution are the same, the ratio i/s is just $\delta + g_{\mathrm{kin}}^{\mathrm{p}}$, and all the treatment applies without any additional problem.

If the plot $1/n_{\mathrm{M}}$ vs g clearly deviates from linearity, and kinetic reasons (i.e. a large variation of $g_{\mathrm{kin}}^{\mathrm{p}}$ with g) can be discarded, it might be that: i) the assumption of having just one ligand with one stability constant is a too crude one for the current system and we have to deal with mixtures; ii) electrostatic effects might be distorting the equations (see section 7, below); iii) ligand excess conditions might not apply; iv) the mild variation of the accumulation with the gel thickness (not far from the analytical error) might preclude any safe treatment of data (especially if sufficient replicates in the same conditions are not available), etc.

It can be shown that, in systems with a finite DBL, eqn. (6) is an excellent approximation for the usual parameters, provided there is an overwhelming contribution of the complex to the total flux in comparison with that of the free metal (i.e. $\varepsilon K' >> 1$).

7. Electrostatic effects

Given that the resin and gel phases include fixed charges in their polymeric structures, electrostatic effects might arise.[56] Potential differences between the resin/gel phases and/or between the gel/solution phases or around the resin beads can develop (i.e. electrostatic potential profiles). When Chelex is used as binding agent, electrostatic effects of the resin are expected to be dominant in comparison to those due to the gel, since the binding sites in the Chelex are charged. Local electrostatic potentials might imply migration terms in the transport equations of charged species. Electrostatic effects will be especially important at low ionic strengths, since otherwise these effects are

436 screened by the salt background. Rigorous solution requires, then, the application of the
437 Nernst-Planck transport equations plus the Poisson equation. This is a cumbersome task,
438 especially for a large number of charged species. A simple situation arises when the
439 electrostatic potential can be considered constant within the solution and resin phases[49]
440 with potential jumps being restricted just at the interfaces (the Donnan potential). This
441 can be a good approximation when the distance between charges is shorter than the Debye
442 length and the influence of the charge of binding species on the Donnan potential is
443 negligible. The Donnan potential difference increases with decreasing ionic strength of
444 the system[2,34] as indicated by the following expression valid for a symmetrical univalent
445 background electrolyte yielding an ionic strength I:

446 $$\Psi_{\text{resin}} - \Psi_{\text{solution}} = \frac{RT}{F} \operatorname{arcsin h}\left(\frac{\rho_{\text{charge,resin}}}{2I} \right) \quad (31)$$

447 where $\rho_{\text{charge,resin}}$ is the charge density in the resin (with its sign). A similar equation can
448 be written between gel and solution when there is a net charge density in the gel.
449 Donnan potential differences lead to Donnan partitioning effects, increasing the
450 concentration of those ions with the opposite charge to that of the phase and decreasing
451 those of the same charge. For instance, at 25ºC, if the gel has a Donnan potential 5 mV
452 more negative than the solution, then a divalent cation at the gel/solution interphase would
453 have an equilibrium concentration at the gel side (designated as $x=(r+g)^{+}$) 1.48 times
454 larger than at the solution side (designated as $x=(r+g)^{-}$) according to the equation:

455 $$\Pi_{r+g,\text{M}} = \frac{c_{\text{M}}^{(r+g)^{+}}}{c_{\text{M}}^{(r+g)^{-}}} = \exp\left(\frac{z_{\text{M}} F \left(\Psi_{\text{gel}} - \Psi_{\text{solution}} \right)}{RT} \right) \quad (32)$$

456 For solutions with just metals, the effect of the charges in the resin is expected to be
457 negligible, since the metal concentration drops to negligible values at the resin-gel
458 interface. However, relevant effects will arise for background cations, anions or charged

459 partially labile complexes. In the latter case, decreasing accumulations or increasing
460 accumulations when ionic strength decreases are expected [43].
461
462 Apart from implying preconcentration or exclusion of the determinand, electrostatic
463 effects might impact on the other species coupled to the analyte. For instance, humic acid
464 enrichment in the gel due to Donnan partitioning could be relevant for metal speciation.[34]
465
466 Donnan partitioning between a typical DGT gel layer and the solution seems to be of
467 limited impact for ionic strength higher than 1 mM,[2] but relevant for doped hydrogels.[57]
468
469 Electrostatic effects seem to be at the root of difficulties in systems with very low ionic
470 strength, such as Canadian lakes.[54] A full consideration of these phenomena, and the
471 consequences for the interpretation of DGT measurements, can be seen in [43]
472

473 ## 8. Limitations and challenges
474

475 The list of issues[2] that can impact on the interpretations and models is large (and cannot
476 be exhaustive): lack of reproducibility in the DBL (changes in δ along the deployment
477 time of one experiment, and from one device to another device); change in the pressure
478 of the layers modifying the diffusion coefficients and their thicknesses; biofouling;[58]
479 different mixtures of ligands and metals changing along the deployment time or from
480 sampling site to sampling site; uncertainty of most parameters (such as diffusion
481 coefficients, tortuosity,[59] DBL thickness..); size discrimination of some complexes or
482 nanoparticles;[60,61] interactions between gels and analytes or ligands;[34,62] lack of

483 uniformity in the distribution of the beads in the resin layer; specificities of the filter;
484 improved geometry including edge effects;[20,63] etc.
485
486 Independent determination of key parameters (e.g. resin capacity and thermodynamic
487 constants,[64,65] etc.) can avoid overparametrization of the models of DGT just based on
488 its own data. Of special relevance is the issue of values of the dissociation rate constants.
489 Usually, Eigen mechanism[66] has been assumed for the complex association rate, so that
490 k_d could be computed from the knowledge of the stability constant. However, especially
491 inside the resin, other kinetic mechanisms (different from the dissociative one) could also
492 be in operation[43].
493
494 There could be an exploitation of the different time-regimes [27] including the initial
495 transient and the final equilibrium stage [16,26].
496
497 Despite the aim of a strong resin with infinity capacity, issues around saturation,
498 competitions by protons (pH effects)[26,32,67] or by different metals[68] need to be fully
499 addressed.
500
501 A complete consideration of the effects and the information obtained with varying some
502 parameter (e.g. the gel thickness,[25,33] the resin thickness,[42,45,46] total metal [44]) could
503 also shed important light on the studied systems.
504
505 The specific characteristics of other sorbent mechanisms (anions, As, etc.) and other
506 interacting phases (such as soils[69,70] or plants[71]) need to be considered and, thus,
507 corresponding models developed or improved.

It is clear, then, that fun in working with the multiple avenues opened by DGT is not going to finish soon.

9. Conclusions

Physicochemical models are essential to interpret DGT results. For instance, eqn. (12) indicates that c_{DGT} is the labile fraction weighted by diffusion coefficients and eqn. (8) is a recipe for computing a lability degree (when the contribution of free metal is negligible) as a normalized flux. Key phenomena identified up to date include: diffusion (in the resin, the gel and the DBL), kinetics of complex association/dissociation, mixture and electrostatic effects. A rigorous, complete, treatment of all these phenomena in an integrated model can only be reached with numerical simulations. However, reasonable assumptions (such as ligand excess, perfect sink for the metal in the resin, one-ligand labilities as surrogate of individual labilities, Donnan partitioning, etc.) allow to reach the model PAM with analytical solutions that: i) lead to a deeper understanding of the impact of the parameters; and ii) facilitate the suggestions of new experimental strategies to derive more robust information from DGT sensors. A crucial point, demanding sound work, is the limitation of the considered phenomena to those strictly required (for a given system), in order to simplify the expressions and be able to access to relevant information without too many unknown parameters.

Apart from dealing rigorously with all cases, numerical simulation also allows for checking the limits of validity of the application of the analytical models. But, both theoretical approaches, analytical and numerical, can only progress if they are also in close contact with experimental realities (including both synthetic solutions and natural samples).

10. Acknowledgments

We thank all our co-workers along these years with DGT and especially to professor William Davison for his inspiration, creativity, kindness and leadership. This study was financially supported by the Spanish Ministry of Education and Science (Project CTM2012-39183) and by the "Comissionat per a Universitats i Recerca del Departament d'Innovació, Universitats i Empresa de la Generalitat de Catalunya"

11. References

[1] W. Davison, H. Zhang, In-situ speciation measurements of trace components in natural- waters using thin-film gels *Nature* **1994**, *367*, 546

[2] W. Davison, H. Zhang, Progress in understanding the use of diffusive gradients in thin films (DGT) – back to basics *Environ. Chem.* **2012**, *9*, 1

[3] L. N. M. Yabuki, C. D. Colaco, A. A. Menegario, R. N. Domingos, C. H. Kiang, D. Pascoaloto, Evaluation of diffusive gradients in thin films technique (DGT) for measuring Al, Cd, Co, Cu, Mn, Ni, and Zn in Amazonian rivers *Environmental Monitoring and Assessment* **2014**, *186*, 961

[4] A. Caillat, P. Ciffroy, M. Grote, S. Rigaud, J. M. Garnier, Bioavailability of Copper in Contaminated Sediments Assessed by A Dgt Approach and the Uptake of Copper by the Aquatic Plant Myriophyllum Aquaticum *Environ. Toxicol. Chem.* **2014**, *33*, 278

[5] D. M. Costello, G. A. Burton, C. R. Hammerschmidt, W. K. Taulbee, Evaluating the performance of Diffusive Gradients in Thin films for predicting ni sediment toxicity *Environ. Sci. Technol.* **2012**, *46*, 10239

[6] F. Degryse, E. Smolders, Cadmium and nickel uptake by tomato and spinach seedlings: plant or transport control? *Environ. Chem.* **2012**, *9*, 48

[7] N. Roig, M. Nadal, J. Sierra, A. Ginebreda, M. Schuhmacher, J. L. Domingo, Novel approach for assessing heavy metal pollution and ecotoxicological status of rivers by means of passive sampling methods *Environ. Int.* **2011**, *37*, 671

[8] V. E. dos Anjos, G. Abate, M. T. Grassi, Comparison of the speciation of trace metals in freshwater employing voltammetry, diffusive gradients in thin films (DGT) and a chemical equilibrium model *Quimica Nova* **2010**, *33*, 1307

[9] O. A. Garmo, N. J. Lehto, H. Zhang, W. Davison, O. Royset, E. Steinnes, Dynamic aspects of DGT as demonstrated by experiments with lanthanide complexes of a multidentate ligand *Environ. Sci. Technol.* **2006**, *40*, 4754

[10] O. A. Garmo, O. Royset, E. Steinnes, T. P. Flaten, Performance study of diffusive gradients in thin films for 55 elements *Anal. Chem.* **2003**, *75*, 3573

[11] S. Tandy, S. Mundus, H. Zhang, E. Lombi, J. Frydenvang, P. E. Holm, S. Husted, A new method for determination of potassium in soils using diffusive gradients in thin films (DGT) *Environ. Chem.* **2012**, *9*, 14

[12] J. G. Panther, P. R. Teasdale, W. W. Bennett, D. T. Welsh, H. J. Zhao, Titanium Dioxide-Based DGT Technique for In Situ Measurement of Dissolved Reactive Phosphorus in Fresh and Marine Waters *Environ. Sci. Technol.* **2010**, *44*, 9419

[13] Y. L. Zhang, S. Mason, A. McNeill, M. J. McLaughlin, Optimization of the diffusive gradients in thin films (DGT) method for simultaneous assay of potassium and plant-available phosphorus in soils *Talanta* **2013**, *113*, 123

[14] J. G. Panther, R. R. Stewart, P. R. Teasdale, W. W. Bennett, D. T. Welsh, H. J. Zhao, Titanium dioxide-based DGT for measuring dissolved As(V), V(V), Sb(V), Mo(VI) and W(VI) in water *Talanta* **2013**, *105*, 80

[15] W. W. Bennett, P. R. Teasdale, D. T. Welsh, J. G. Panther, R. R. Stewart, H. L. Price, D. F. Jolley, Inorganic arsenic and iron(II) distributions in sediment porewaters investigated by a combined DGT-colourimetric DET technique *Environ. Chem.* **2012**, *9*, 31

[16] H. P. van Leeuwen, Steady-state DGT fluxes of nanoparticulate metal complexes *Environ. Chem.* **2011**, *8*, 525

[17] E. Navarro, F. Piccapietra, B. Wagner, F. Marconi, R. Kaegi, N. Odzak, L. Sigg, R. Behra, Toxicity of Silver Nanoparticles to Chlamydomonas reinhardtii *Environ. Sci. Technol.* **2008**, *42*, 8959

[18] C. E. Chen, H. Zhang, G. G. Ying, K. C. Jones, Evidence and Recommendations to Support the Use of a Novel Passive Water Sampler to Quantify Antibiotics in Wastewaters *Environ. Sci. Technol.* **2013**, *47*, 13587

[19] W. Davison, G. Fones, M. Harper, P. Teasdale, H. Zhang, in *In situ monitoring of aquatic systems* (Eds J. Buffle, G. Horvai) **2000,** pp.495-569 (John Wiley: Chichester, UK).

[20] M. P. Harper, W. Davison, W. Tych, Temporal, spatial, and resolution constraints for in situ sampling devices using diffusional equilibration: Dialysis and DET *Environ. Sci. Technol.* **1997**, *31*, 3110

[21] H. Ernstberger, W. Davison, H. Zhang, A. Tye, S. Young, Measurement and dynamic modeling of trace metal mobilization in soils using DGT and DIFS *Environ. Sci. Technol.* **2002**, *36*, 349

[22] M. H. Tusseau-Vuillemin, R. Gilbin, M. Taillefert, A dynamic numerical model to characterize labile metal complexes collected with diffusion gradient in thin films devices *Environ. Sci. Technol.* **2003**, *37*, 1645

[23] F. Degryse, E. Smolders, R. Merckx, Labile Cd complexes increase Cd availability to plants *Environ. Sci. Technol.* **2006**, *40*, 830

[24] N. J. Lehto, W. Davison, H. Zhang, W. Tych, An evaluation of DGT performance using a dynamic numerical model *Environ. Sci. Technol.* **2006**, *40*, 6368

[25] J. L. Levy, H. Zhang, W. Davison, J. Galceran, J. Puy, Kinetic Signatures of Metals in the Presence of Suwannee River Fulvic Acid *Environ. Sci. Technol.* **2012**, *46*, 3335

[26] S. Mongin, R. Uribe, C. Rey-Castro, J. Cecilia, J. Galceran, J. Puy, Limits of the Linear Accumulation Regime of DGT Sensors *Environ. Sci. Technol.* **2013**, *47*, 10438

[27] J. Puy, R. Uribe, S. Mongin, J. Galceran, J. Cecilia, J. Levy, H. Zhang, W. Davison, Lability Criteria in Diffusive Gradients in Thin Films *J. Phys. Chem. A* **2012**, *116*, 6564

[28] J. Galceran, J. Puy, J. Salvador, J. Cecília, H. P. van Leeuwen, Voltammetric lability of metal complexes at spherical microelectrodes with various radii *J. Electroanal. Chem.* **2001**, *505*, 85

[29] D. Alemani, J. Buffle, Z. Zhang, J. Galceran, B. Chopard, Metal flux and dynamic speciation at (bio)interfaces. Part III: MHEDYN, a general code for metal flux computation; application to simple and fulvic complexants *Environ. Sci. Technol.* **2008**, *42*, 2021

[30] R. Uribe, J. Puy, J. Cecilia, J. Galceran, Kinetic Mixture Effects in Diffusion Gradients in Thin Films (DGT) *Phys. Chem. Chem. Phys.* **2013**, *15*, 11349

[31] J. Galceran, J. Puy, J. Salvador, J. Cecília, F. Mas, J. L. Garcés, Lability and mobility effects on mixtures of ligands under steady-state conditions *Phys. Chem. Chem. Phys.* **2003**, *5*, 5091

[32] H. Zhang, W. Davison, Performance-characteristics of diffusion gradients in thin- films for the in-situ measurement of trace-metals in aqueous- solution. *Anal. Chem.* **1995**, *67*, 3391

[33] K. W. Warnken, W. Davison, H. Zhang, J. Galceran, J. Puy, In situ measurements of metal complex exchange kinetics in freshwater *Environ. Sci. Technol.* **2007**, *41*, 3179

[34] P. L. R. van der Veeken, H. P. van Leeuwen, Gel-water partitioning of soil humics in diffusive gradient in thin film (DGT) analysis of their metal complexes *Environ. Chem.* **2012**, *9*, 24

[35] E. R. Unsworth, K. W. Warnken, H. Zhang, W. Davison, F. Black, J. Buffle, J. Cao, R. Cleven, J. Galceran, P. Gunkel, E. Kalis, D. Kistler, H. P. van Leeuwen, M. Martin, S. Noel, Y. Nur, N. Odzak, J. Puy, W. H. van Riemsdijk, L. Sigg, E. Temminghoff, M. L. Tercier-Waeber, S. Toepperwien, R. M. Town, L. P. Weng, H. B. Xue, Model predictions of metal speciation in freshwaters compared to measurements by in situ techniques *Environ. Sci. Technol.* **2006**, *40*, 1942

[36] N. Serrano, J. M. Díaz-Cruz, C. Ariño, M. Esteban, J. Puy, E. Companys, J. Galceran, J. Cecilia, Full-wave analysis of stripping chronopotentiograms at scanned deposition potential (SSCP) as a tool for heavy metal speciation: Theoretical development and application to Cd(II)-phthalate and Cd(II)-iodide systems *J. Electroanal. Chem.* **2007**, *600*, 275

[37] L. Six, E. Smolders, R. Merckx, The performance of DGT versus conventional soil phosphorus tests in tropical soils-maize and rice responses to P application *Plant Soil* **2013**, *366*, 49

[38] S. C. Apte, G. E. Batley, K. C. Bowles, P. L. Brown, N. Creighton, L. T. Hales, R. V. Hyne, M. Julli, S. I. Markich, F. Pablo, N. J. Rogers, J. L. Stauber, K. Wilde, A comparison of copper speciation measurements with the toxic responses of three sensitive freshwater organisms *Environ. Chem.* **2005**, *2*, 320

[39] J. Salvador, J. Puy, J. Cecilia, J. Galceran, Lability of complexes in steady state finite planar diffusion *J. Electroanal. Chem.* **2006**, *588*, 303

[40] S. Mongin, R. Uribe, J. Puy, J. Cecilia, J. Galceran, H. Zhang, W. Davison, Key Role of the Resin Layer Thickness in the Lability of Complexes Measured by DGT *Environ. Sci. Technol.* **2011**, *45*, 4869

[41] R. Uribe, S. Mongin, J. Puy, J. Cecilia, J. Galceran, H. Zhang, W. Davison, Contribution of Partially Labile Complexes to the DGT Metal Flux *Environ. Sci. Technol.* **2011**, *45*, 5317

[42] J. L. Levy, H. Zhang, W. Davison, J. Puy, J. Galceran, Assessment of trace metal binding kinetics in the resin phase of diffusive gradients in thin films *Anal. Chim. Acta* **2012**, *717*, 143

[43] J. Puy, J. Galceran, S. Cruz-Gonzalez, C. A. David, R. Uribe, C. Lin et al.,Metal accumulation in DGT: Impact of ionic strength and kinetics of dissociation of complexes in the resin domain *Anal Chem* **2014** Submitted.

[44] R. M. Town, P. Chakraborty, H. P. van Leeuwen, Dynamic DGT speciation analysis and applicability to natural heterogeneous complexes *Environ. Chem.* **2009**, *6*, 170

[45] M. R. S. Arvajeh, N. Lehto, O. A. Garmo, H. Zhang, Kinetic Studies of Ni Organic Complexes Using Diffusive Gradients in Thin Films (DGT) with Double Binding Layers and a Dynamic Numerical Model *Environ. Sci. Technol.* **2013**, *47*, 463

[46] N. J. Lehto, W. Davison, H. Zhang, The use of ultra-thin diffusive gradients in thin-films (DGT) devices for the analysis of trace metal dynamics in soils and sediments: a measurement and modelling approach *Environ. Chem.* **2012**, *9*, 415

[47] J. Salvador, J. L. Garcés, E. Companys, J. Cecilia, J. Galceran, J. Puy, R. M. Town, Ligand mixture effects in metal complex lability *J. Phys. Chem. A* **2007**, *111*, 4304

[48] Z. S. Zhang, J. Buffle, R. M. Town, J. Puy, H. P. van Leeuwen, Metal Flux in Ligand Mixtures. 2. Flux Enhancement Due to Kinetic Interplay: Comparison of the Reaction Layer Approximation with a Rigorous Approach *J. Phys. Chem. A* **2009**, *113*, 6572

[49] H. P. van Leeuwen, J. Galceran, in *Physicochemical kinetics and transport at chemical-biological surfaces* (Eds H. P. van Leeuwen, W. Koester) **2004,** pp.113-146 (John Wiley: Chichester, UK).

[50] O. A. Garmo, K. R. Naqvi, O. Royset, E. Steinnes, Estimation of diffusive boundary layer thickness in studies involving diffusive gradients in thin films (DGT) *Anal. Bioanal. Chem.* **2006**, *386*, 2233

[51] E. Uher, M. H. Tusseau-Vuillemin, C. Gourlay-France, DGT measurement in low flow conditions: diffusive boundary layer and lability considerations *Environmental Science-Processes & Impacts* **2013**, *15*, 1351

[52] H. Zhang, W. Davison, R. Gadi, T. Kobayashi, In situ measurement of dissolved phosphorus in natural waters using DGT *Anal. Chim. Acta* **1998**, *370*, 29

[53] G. S. C. Turner, G. A. Mills, M. J. Bowes, J. L. Burnett, S. Amos, G. R. Fones, Evaluation of DGT as a long-term water quality monitoring tool in natural waters; uranium as a case study *Environmental Science-Processes & Impacts* **2014**, *16*, 393

[54] M. Alfaro-De la Torre, P. Y. Beaulieu, A. Tessier, In situ measurement of trace metals in lakewater using the dialysis and DGT techniques *Anal. Chim. Acta* **2000**, *418*, 53

[55] K. W. Warnken, H. Zhang, W. Davison, Accuracy of the diffusive gradients in thin-films technique: Diffusive boundary layer and effective sampling area considerations *Anal. Chem.* **2006**, *78*, 3780

[56] N. Fatin-Rouge, A. Milon, J. Buffle, R. R. Goulet, A. Tessier, Diffusion and partitioning of solutes in agarose hydrogels: The relative influence of electrostatic and specific interactions *J. Phys. Chem. B* **2003**, *107*, 12126

[57] L. P. Yezek, P. L. R. van der Veeken, H. P. van Leeuwen, Donnan Effects in Metal Speciation Analysis by DET/DGT *Environ. Sci. Technol.* **2008**, *42*, 9250

[58] E. Uher, H. Zhang, S. Santos, M. H. Tusseau-Vuillemin, C. Gourlay-France, Impact of Biofouling on Diffusive Gradient in Thin Film Measurements in Water *Anal. Chem.* **2012**, *84*, 3111

[59] E. J. M. Temminghoff, A. C. C. Plette, R. van Eck, W. H. van Riemsdijk, Determination of the chemical speciation of trace metals in aqueous systems by the Wageningen Donnan Membrane Technique *Anal. Chim. Acta* **2000**, *417*, 149

[60] N. Fatin-Rouge, K. Starchev, J. Buffle, Size effects on diffusion processes within agarose gels *Biophys. J.* **2004**, *86*, 2710

[61] P. L. R. van der Veeken, J. P. Pinheiro, H. P. van Leeuwen, Metal Speciation by DGT/DET in Colloidal Complex Systems *Environ. Sci. Technol.* **2008**, *42*, 8835

[62] O. A. Garmo, W. Davison, H. Zhang, Effects of Binding of Metals to the Hydrogel and Filter Membrane on the Accuracy of the Diffusive Gradients in Thin Films Technique *Anal. Chem.* **2008**, *80*, 9220

[63] Garmo OA **Using a dynamic numerical model to simulate the effects of lateral diffusion and diffusive boundary layer on uptake in different types of DGT devices**. Conference on DGT and the Environment. Lancaster (United Kingdom): 2013.

[64] G. Alberti, R. Biesuz, Empore (TM) membrane vs. Chelex 100: Thermodynamic and kinetic studies on metals sorption *Reactive & Functional Polymers* **2011**, *71*, 588

[65] M. Pesavento, R. Biesuz, M. Gallorini, A. Profumo, Sorption mechanism of trace amounts of divalent metal-ions on a chelating resin containing iminodiacetate groups *Anal. Chem.* **1993**, *65*, 2522

[66] F. M. M. Morel, J. G. Hering, in *Principles and Applications of Aquatic Chemistry* **1993,** pp.319-420 (John Wiley: New York).

[67] J. Gimpel, H. Zhang, W. Hutchinson, W. Davison, Effect of solution composition, flow and deployment time on the measurement of trace metals by the diffusive gradient in thin films technique *Anal. Chim. Acta* **2001**, *448*, 93

[68] F. Degryse, E. Smolders, I. Oliver, H. Zhang, Relating soil solution Zn concentration to diffusive gradients in thin films measurements in contaminated soils *Environ. Sci. Technol.* **2003**, *37*, 3958

[69] M. P. Harper, W. Davison, W. Tych, DIFS - a modelling and simulation tool for DGT induced trace metal remobilisation in sediments and soils *Environmental Modelling & Software* **2000**, *15*, 55

[70] F. Degryse, E. Smolders, H. Zhang, W. Davison, Predicting availability of mineral elements to plants with the DGT technique: a review of experimental data and interpretation by modelling *Environ. Chem.* **2009**, *6*, 198

[71] D. Ferreira, P. Ciffroy, M. H. Tusseau-Vuillemin, A. Bourgeault, J. M. Gamier, DGT as surrogate of biomonitors for predicting the bioavailability of copper in freshwaters: An ex situ validation study *Chemosphere* **2013**, *91*, 241

12. Tables

Table 1 Hypothetical systems consisting of a metal M and two ligand ^{1}L and ^{2}L sharing the same total metal concentration (10.02 nM), the same free metal concentration (0.02 nM) and resulting in a common expected c_{DGT} (5.02 nM), despite the very different nature of the relevant physicochemical processes.

ξ_1	ε_1	$c^*_{M^1L}$ / nM	ξ_2	ε_2	$c^*_{M^2L}$ / nM	contrib 1[a)] / nM	contrib 2 [a)] / nM	c_{DGT} / nM
0.5	1	5	1	0.50	5	2.5	2.5	5.02
1	1	5	1	0	5	5	0	5.02
0	1	5	1	1	5	0	5	5.02
1	1.4	3	0.82	0.14	7	4.2	0.80	5.02

Foot to table : $\varepsilon_j \equiv \frac{D_{M^jL}}{D_M}$. a) Contrib. 1 or 2: Contribution of complex M^jL to c_{DGT}, computed as $\xi_j \frac{D_{M^jL}}{D_M} c^*_{M^jL}$

Table 2 Numerical values of parameters in the figures.

parameter	value
$c^*_{T,Cd}$	10^{-2} mol m^{-3}
$c^*_{T,Co}$	10^{-2} mol m^{-3}
$c^*_{T,Ni}$	2.5×10^{-2} mol m^{-3}
D_M (in gel)	$0.8\times D^w_M$
D^w_{Cd}	6.85×10^{-10} m^{2}s^{-1}
D^w_{Co}	6.68×10^{-10} m^{2}s^{-1}
D^w_{Ni}	7.07×10^{-10} m^{2}s^{-1}
$D_{M\text{-}NTA}$ (in gel and resin)	εD_M
$D^w_{M\text{-}NTA}$	$\varepsilon^w D^w_{Co}$
g	8.52×10^{-3} m
$k_{d,Cd}$	4.19 s^{-1}
$k_{d,Co}$	0.00783 s^{-1}
$k_{d,Ni}$	7.7×10^{-6} s^{-1}
K' for Cd	1080
K' for Co	4490
K' for Ni	60600
r	4×10^{-4} m
δ	1×10^{-4} m
$\varepsilon=\varepsilon^w$	0.7

776 # 13. Figures

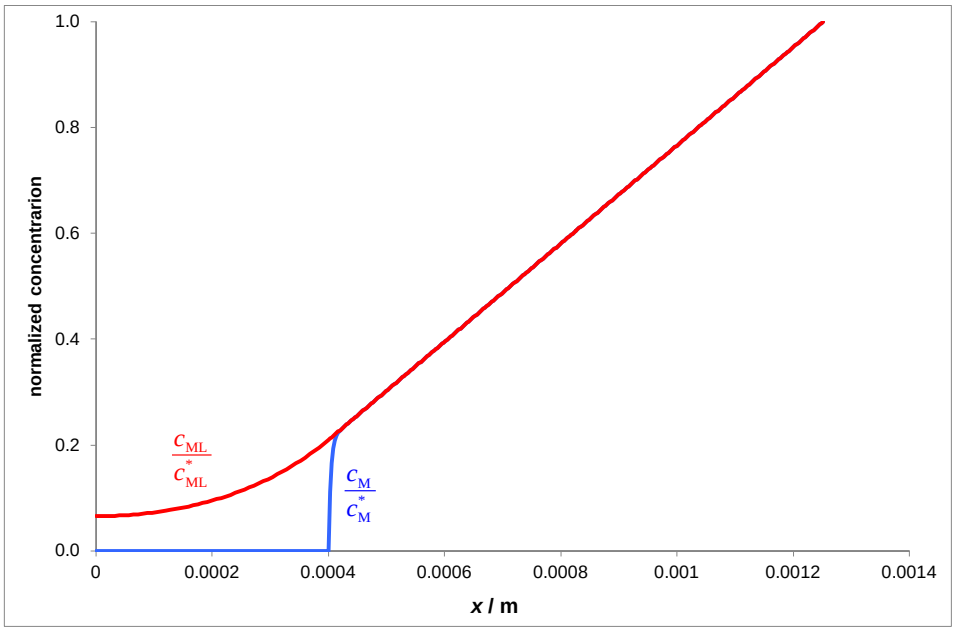

777

778 *Fig 1: Normalized concentration profiles of CoNTA with parameters in Table 2.*

779

780

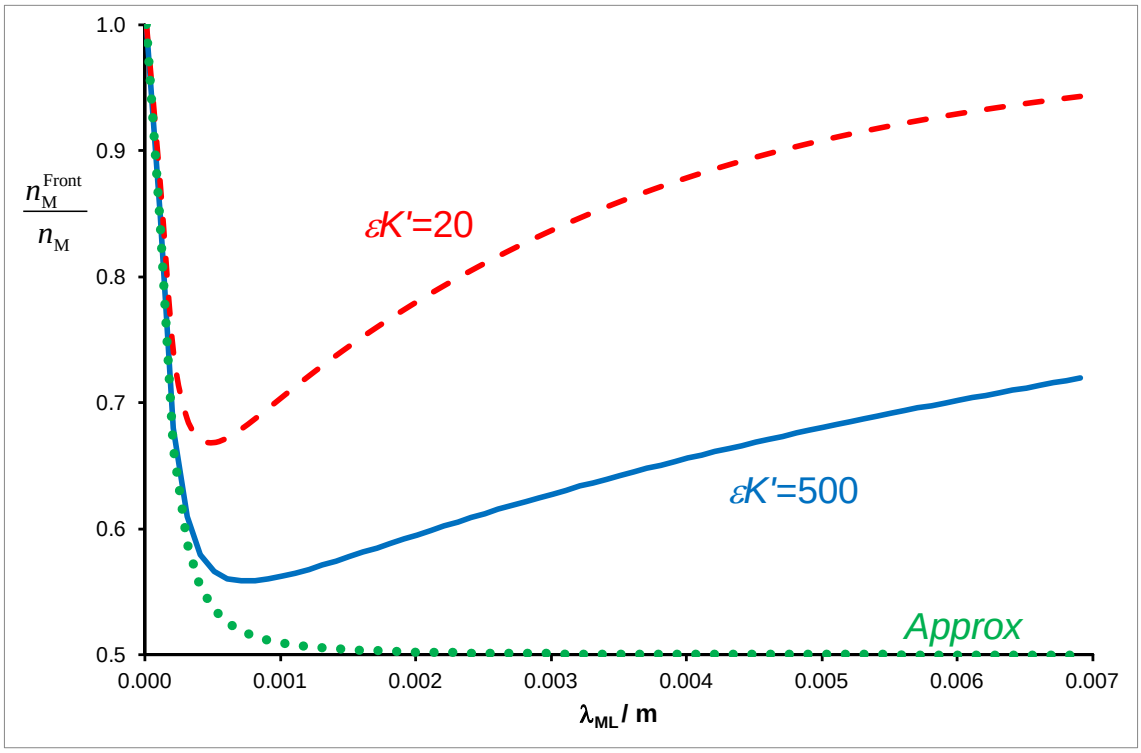

781
782

783 *Fig 2: Ratio of accumulated number of moles of a metal M for different complexes with varying lability*
784 *(from high lability at the left to low lability at the right) between the front layer (of thickness r/2) and*
785 *the total number of moles accumulated by both binding layers. Rigorous expression (23) is used for*
786 *εK'=500 in blue continuous line and for εK'=20 in red dashed line. Approximate expression (24) is*
787 *plotted in green dotted line. Other parameters: g= 8.52 ×10⁻⁴ m; r=4 ×10⁻⁴ m.*

788
789

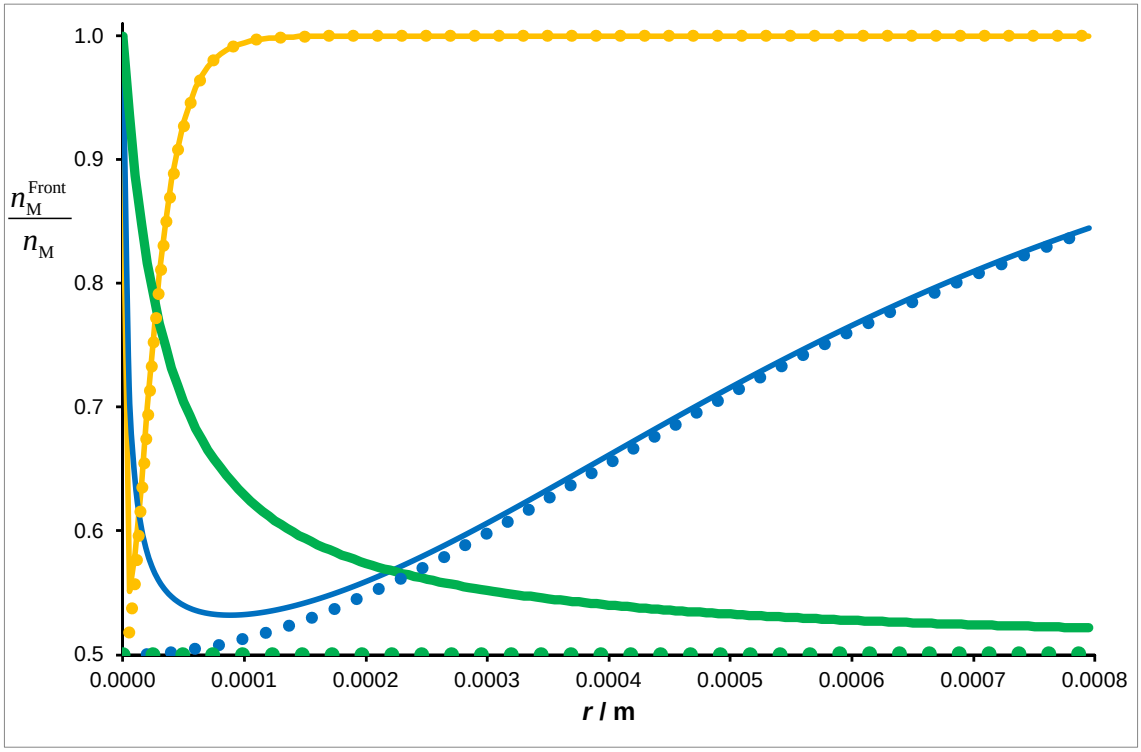

Fig 3: Ratio of moles of Cd (orange continuous line), Co (blue continuous line) or Ni (green continuous line) accumulated in the front layer with respect to the total number of moles accumulated in both layers vs. the total thickness of the resin ensemble computed with the rigorous expression (23). Values computed with the approximate expression (24) are represented as dotted lines in the same colour (for the case of Ni it is almost on top of the abscissae axis). Other parameters as in Table 2.

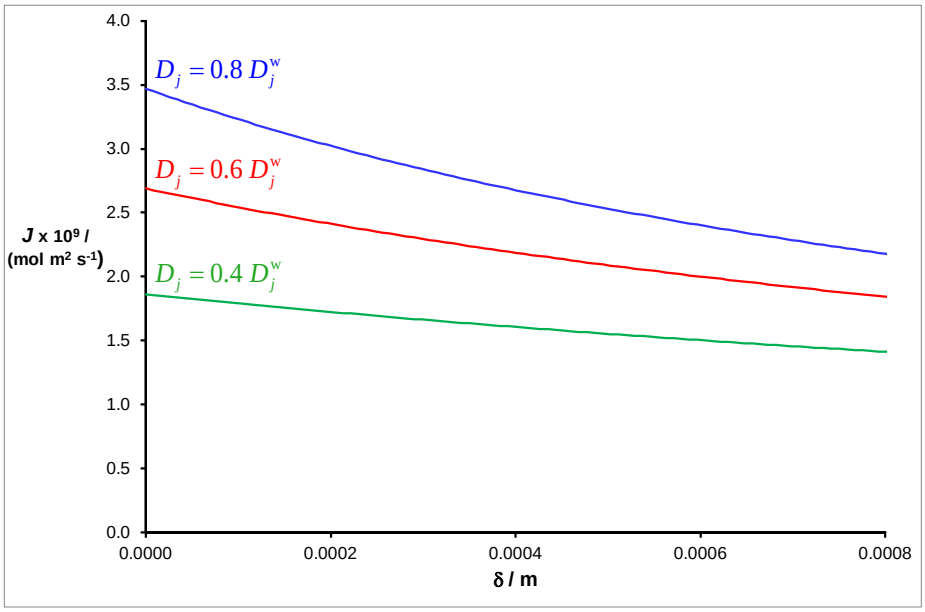

,

Fig 4: Impact of varying DBL thickness (δ) on the total flux of Co obtained in a system with one complex (CoNTA) as computed with the Penetration Analytical Model without electrostatic effects. The 3 lines stand for different reductions[34] (80%, 60% and 40%) in the diffusion coefficients of all species when entering the gel (with respect to an aqueous solution). See other parameters in Table 2.

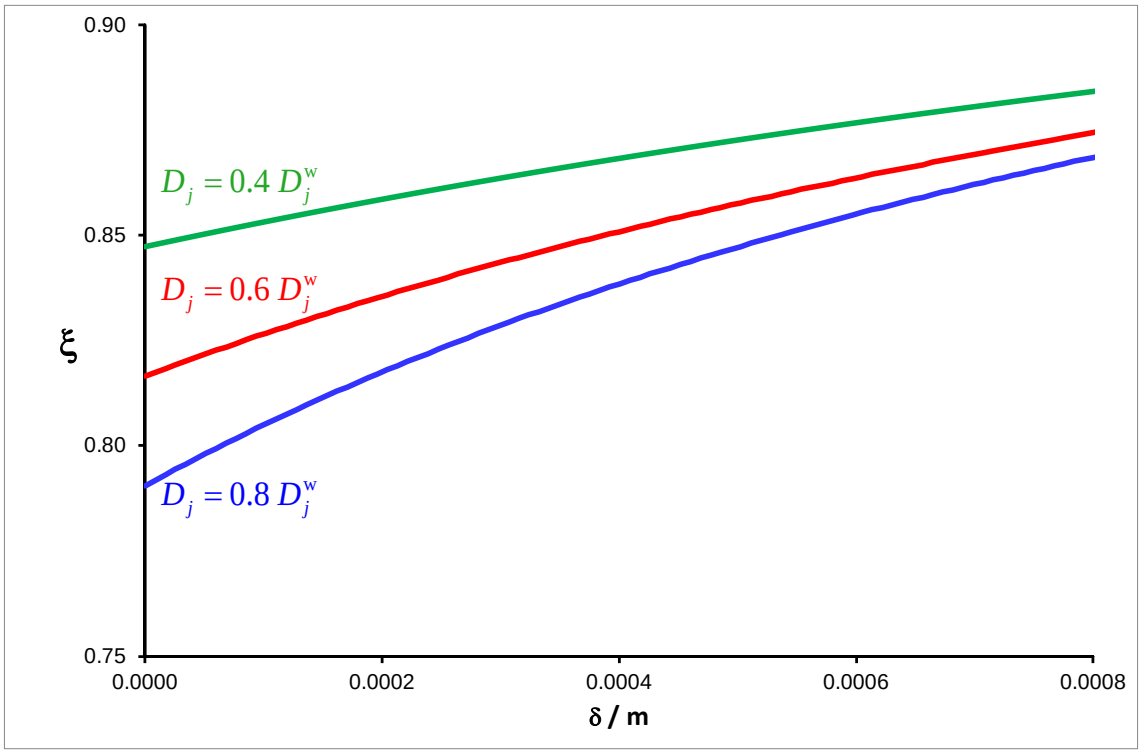

807

808 *Fig 5: Impact of varying DBL thickness (δ) on the lability degree of CoNTA taking into account the*
809 *penetration into the resin. Conditions and parameters as in Fig 4.*
810

811

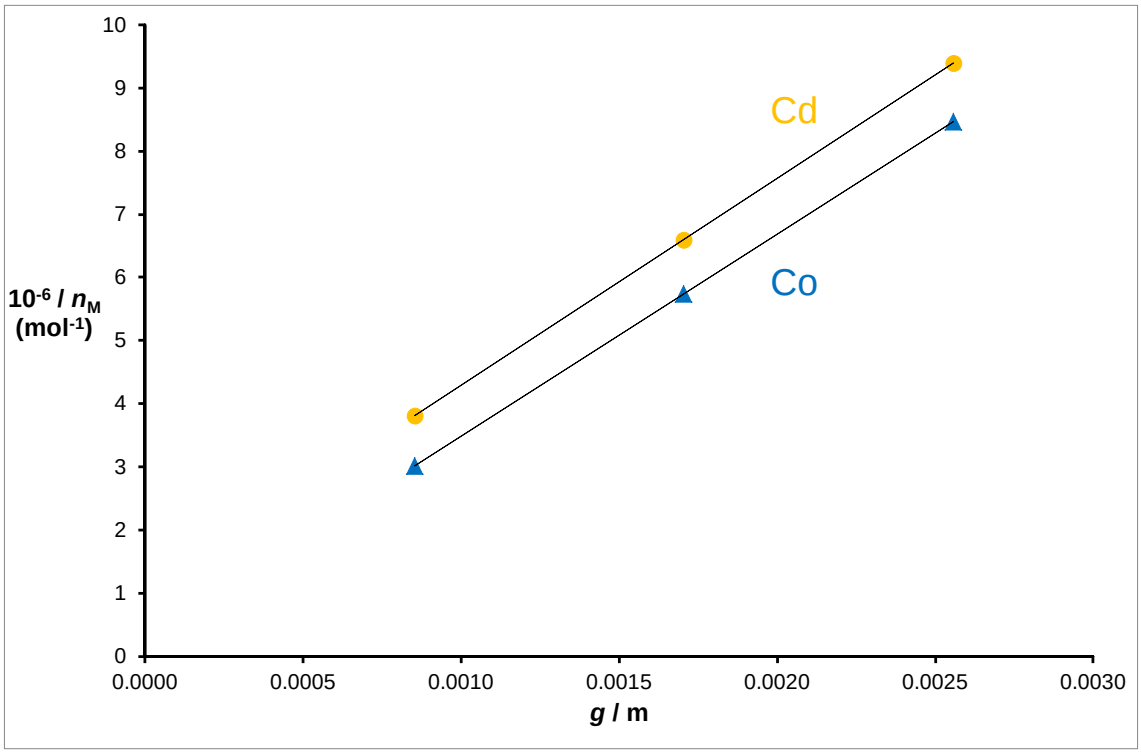

Fig 6: Plot of the inverse of the mass accumulated for increasing gel thicknesses in a system with CdNTA (orange circle markers) and CoNTA (blue triangle markers), showing a good linearity for these synthetic data (using one, two and three gels of thickness 8.52×10^{-4} m). This plot would allow the successful recovery of the kinetics parameters of CoNTA and CdNTA with eqn 30 if all other parameter values were known. Area= 3.14×10^{-4} m; time= 3 days. Other parameters as in table 2.